



# Numerical investigation of blood flow in a deformable coronary bifurcation and non-planar branch

Seyed Esmail Razavi<sup>1,2\*</sup>, Amir Ali Omid<sup>3</sup>, Massoud Saghafi Zanjani<sup>1\*</sup>

<sup>1</sup> Faculty of Mechanical Engineering, University of Tabriz, Tabriz, Iran

<sup>2</sup> Research Center for Pharmaceutical Nanotechnology, Tabriz University of Medical Sciences, Tabriz Iran

<sup>3</sup> Faculty of Electrical and Computer Engineering, University of Tabriz, Tabriz, Iran

## Article Info



### Article Type:

Research Article

### Article History:

Received: 08 Nov. 2014

Revised: 20 Dec. 2014

Accepted: 27 Dec. 2014

ePublished: 30 Dec. 2014

### Keywords:

Coronary bifurcation  
 Numerical investigation  
 Pulsatile flow  
 Non-planar bifurcation  
 Elastic wall  
 Coronary artery disease

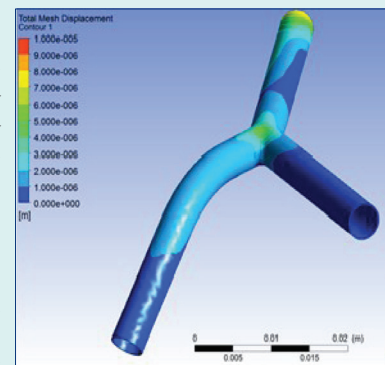
## Abstract

**Introduction:** Among cardiovascular diseases, arterials stenosis is recognized more commonly than the others. Hemodynamic characteristics of blood play a key role in the incidence of stenosis. This paper numerically investigates the pulsatile blood flow in a coronary bifurcation with a non-planar branch. To create a more realistic analysis, the wall is assumed to be compliant. Furthermore, the flow is considered to be three-dimensional, incompressible, and laminar.

**Methods:** The effects of non-Newtonian blood, compliant walls and different angles of bifurcation on hemodynamic characteristics of flow were evaluated. Shear thinning of blood was simulated with the Carreau-Yasuda model. The current research was mainly focused on the flow characteristics in bifurcations since atherosclerosis occurs mostly in bifurcations. Moreover, as the areas with low shear stresses are prone to stenosis, these areas were identified.

**Results:** Our findings indicated that the compliant model of the wall, bifurcation's angle, and other physical properties of flow have an impact on hemodynamics of blood flow. Lower wall shear stress was observed in the compliant wall than that in the rigid wall. The outer wall of bifurcation in all models had lower wall shear stress. In bifurcations with larger angles, wall shear stress was higher in outer walls, and lower in inner walls.

**Conclusion:** The non-Newtonian blood vessels and different angles of bifurcation on hemodynamic characteristics of flow evaluation confirmed a lower wall shear stress in the compliant wall than that in the rigid wall, while the wall shear stress was higher in outer walls but lower in inner walls in the bifurcation regions with larger angles.



## Introduction

Identification and assessment of hemodynamic characteristics and other properties of flow have an impact on the treatment and prevention of cardiovascular diseases. Stenosis and atherosclerosis are highly dependent on the local hemodynamic characteristics of blood flow.<sup>1-4</sup> Since coronary artery diseases are associated with high rate of mortality and morbidity, the hemodynamic characteristics of blood flow demands more attention. On the other hand, intimal hyperplasia and failure of bypass surgery are highly dependent on these characteristics.<sup>5</sup> Factors such as low shear stress,<sup>6,7</sup> low shear rate, abnormality of blood flow,<sup>8</sup> and temporal changes of shear stress can lead to stenosis and atherosclerosis. The vessel geometry can also play an important role in the formation of atherosclerosis plaques.<sup>9</sup>

The atherosclerosis plaques usually take place in curvatures, bifurcations and vessel branches.<sup>10,11</sup> Non planarity of artery bifurcation has an efficient role on the characteristics of flow.<sup>12</sup> In addition to these factors, pulsatile flow can have a substantial effect on the hemodynamic characteristics of blood.<sup>7</sup> A number of investigations have been conducted on the blood flow in the coronary bifurcations. For instance, Perktold and Peter<sup>13</sup> investigated the pulsatile blood flow in a 90 °T-bifurcation artery model. The nonlinear Navier-Stokes equations for time-dependent incompressible Newtonian fluid flow were solved using the finite element method. It was found that atherosclerotic lesions were localized at the outer walls of bifurcations and T-junctions.

Prosi et al<sup>14</sup> numerically analyzed the influence of dynamic curvature on the coronary artery hemodynamics using the

\*Corresponding authors: Seyed Esmail Razavi, Email: [razavi@tabrizu.ac.ir](mailto:razavi@tabrizu.ac.ir); Massoud Saghafi Zanjani, Email: [massoud.saghafi@gmail.com](mailto:massoud.saghafi@gmail.com)



© 2014 The Author(s). This work is published by BioImpacts as an open access article distributed under the terms of the Creative Commons Attribution License (<http://creativecommons.org/licenses/by-nc/4.0/>). Non-commercial uses of the work are permitted, provided the original work is properly cited.

finite element method. They used a realistic model of the coronary artery bifurcation and its first diagonal branch was curved by attaching it to the surface of a sphere with time-varying radius, based on experimental dynamic curvature data. Near the branching, the effect of out-of-plane curvature on the bifurcation flow was modest. Downstream of the bifurcation, the influence of curvature increased, resulting in a stronger skewing of the velocity profiles towards the pericardial wall; however, only minor influences of curvature dynamics on the flow field were observed.

Sun et al.<sup>15</sup> investigated the hemodynamic effect of variations in the angulations of the left coronary artery, based on simulated and realistic coronary artery models. Twelve models consisting of four realistic and eight simulated coronary artery geometries were generated with the inclusion of left main stem, left anterior descending, and left circumflex branches. The wall shear stress, wall shear stress gradient, velocity flow patterns and wall pressure were measured in simulated and realistic models during the cardiac cycle. The results showed that there is a direct correlation between coronary angulations and subsequent hemodynamic changes, based on the realistic and simulated models. A disturbed flow pattern was observed in models with wider angulations, and a low wall shear stress gradient was demonstrated in the inner wall of bifurcation with wide angles.

In all of these works the vessel wall is assumed to be rigid, and to the author's knowledge, little works have been done to investigate the compliant model of the wall. Due to the difficulties of coupled fluid and solid problems, in most of the works the model wall is assumed to be rigid. But in reality, the walls of arteries are deformable and interact with pulsatile blood flow. It means that hemodynamic characteristics of blood flow are influenced by mechanics of vessel wall, and dynamic properties of the wall are also influenced by treatment of blood flow.<sup>16</sup>

In this work, the blood flow in coronary artery bifurcation with a non-planar branch has been investigated. The vessel wall is considered as linear elastic, and non-Newtonian and Newtonian flow cases are considered. The effects of wall compliance and non-Newtonian rheology of blood on characteristics of the flow have been studied. Also the effect of bifurcation angle on flow behavior is investigated.

### Computational Procedure

For coupling the results of solid and fluid parts, an iterative method was used. Firstly, fluid pressure at different points is calculated, and with the pressure at the fluid boundary, displacement of the solid wall was found. Then, this displacement is applied to the moving mesh in the fluid and fluid pressure is recalculated. This cycle was repeated until the following criterion was met:

$$C = \max \left( \frac{|d_i^{n+1} - d_i^n|}{|d_i^{n+1}|} \right) \leq C_{crt} \quad (1)$$

Where  $d_i^n$  is the displacement of the node  $I$  at  $n$  iterations, and  $C_{crt}$  the convergence criterion. The convergence of pressure field is fulfilled in a similar manner.

### Vessel geometry

In the current study, a coronary artery bifurcation with a non-planar branch was simulated. For this purpose, the three-dimensional model of Chen and Lu<sup>9</sup> was used. In this model, all vessels have the same diameters ( $D$ ). The length of the mother vessel was considered  $3D$  before the bifurcation. In the bifurcation point, mother vessel was divided into two daughter vessels. In the main model, the bifurcation angle is  $90^\circ$ . One of the daughter vessels after the length of  $1.5D$ , with a curvature angle of  $45^\circ$  and radius of  $4D$  gets out of the main plane and continues with the length of  $4D$ . Other branch of bifurcation continues with the length of  $8D$  in the main plane. In the present work, the vessel diameter was considered  $4\text{mm}$ , and other characteristics were similar to the mentioned model, except a difference in having the fully developed flow before bifurcation. The length of the mother vessel was longer ( $40\text{ mm}$ ) than that of the main model ( $12\text{ mm}$ ). Different bifurcation angles were considered  $90^\circ$ ,  $75^\circ$  and  $65^\circ$ . Fig. 1 shows the  $90^\circ$  bifurcation as well as different lines on it. These lines are used to compare the results.

The vessel was considered to be isotropic, incompressible and homogenous with the density of  $1060 \frac{\text{kg}}{\text{m}^3}$  and the vessel wall was assumed linear elastic.<sup>17</sup> The Poisson ratio was taken to be  $\nu \approx 0.5$  to express the incompressibility of the isotropic vessel wall material.<sup>17</sup> The elastic moduli (Young's modulus) of vessel wall at mean physiological pressure was regarded as  $E=2.2\text{ Mpa}$ .<sup>17</sup> The transient equilibrium equation for the vessel wall read:

$$\{F_{(t)}\} = [M] \{\ddot{u}_{(t)}\} + [K] \{u_{(t)}\} \quad (2)$$

where,  $\{F\}$  is the load vector,  $[M]$  is the structural mass matrix,  $[K]$  is the structural stiffness matrix,  $\{u\}$  is the nodal displacement vector, and  $\{\ddot{u}\}$  is the nodal acceleration vector.

These equations were solved by a finite element method. The wall thickness of the anterior descending artery was provided by Gradus-Pizlo to be  $t=1.9 \pm 0.3\text{ mm}$ .<sup>18</sup> Accordingly, the wall thickness of both the graft and artery was taken to be  $2\text{ mm}$  in this investigation though it may impose somewhat uncertainty.

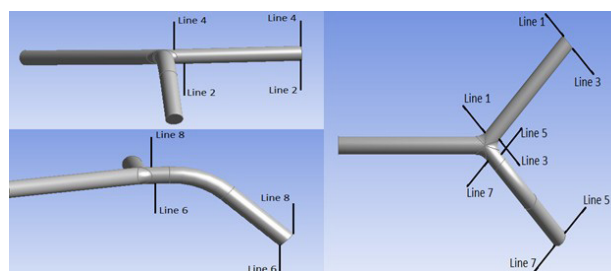


Fig. 1. Model geometry and different lines on it

**Blood Flow Model**

The flow was assumed to be three-dimensional, incompressible and laminar. The continuity and momentum equations are as follows:

$$\frac{d}{dt} \int_{V(t)} \rho dV + \int_s \rho(\bar{u} - \bar{u}_g) \cdot d\bar{A} = 0 \tag{3}$$

$$\frac{d}{dt} \int_{V(t)} \rho \bar{u} dV + \int_s \rho(\bar{u} - \bar{u}_g) \bar{u} \cdot d\bar{A} = - \int_s P d\bar{A} + \int_s \eta \left( \frac{\partial u_i}{\partial x_j} + \frac{\partial u_j}{\partial x_i} \right) d\bar{A} \tag{4}$$

where,  $\rho$  is fluid density,  $\bar{u}$  is flow velocity vector and  $\bar{u}_g$  is the velocity of the control volume boundary (grid velocity). The blood density was taken to be  $1050 \frac{kg}{m^3}$ .<sup>17</sup> These equations were solved by a control volume method with ANSYS CFX software. Shear thinning of blood is evaluated by Carreau-Yasuda model,<sup>17</sup> as follows:

$$\eta = \eta_{\infty} + (\eta_0 - \eta_{\infty}) [1 + \lambda \dot{\gamma}^a]^{-n}; \dot{\gamma} = \sqrt{2tr(D^2)} \tag{5}$$

where,  $\dot{\gamma}$  is the rate of deformation tensor ( $D = \frac{[\nabla U + (\nabla U)^T]}{2}$ ).

Other parameters were obtained from the experimental data of Gijssen et al<sup>19</sup> which included:  $\eta_0 = 22 \times 10^{-3}$  Pa s,  $\eta_{\infty} = 2.2 \times 10^{-3}$  Pa s,  $\lambda = 0.11$  s,  $a = 0.644$  and  $n = 0.392$ . In the case of Newtonian flow, the dynamic viscosity of blood was taken to be  $\eta = 0.0035$  Pas. The flow at the inlet of mother vessel was considered pulsatile with a periodicity of  $T = 0.8$  s as shown in Fig. 2. Velocity was measured by phase contrast MRI technique by a research group at University of Illinois, Chicago.<sup>20</sup> The Reynolds number for the Newtonian fluid flow, varies from about 230 (diastole) to 408 (peak systole).

The zero absolute pressure was used at the outlet boundary condition,<sup>9</sup> and no slip condition was used at the walls. The convergence criterion was set to be  $10^{-5}$ .<sup>17</sup> The mesh independence was tested on the velocity and wall shear stress (WSS) (Table 1). The time-step size was taken to be 0.01 s,<sup>17</sup> and the results were recorded at the end of each

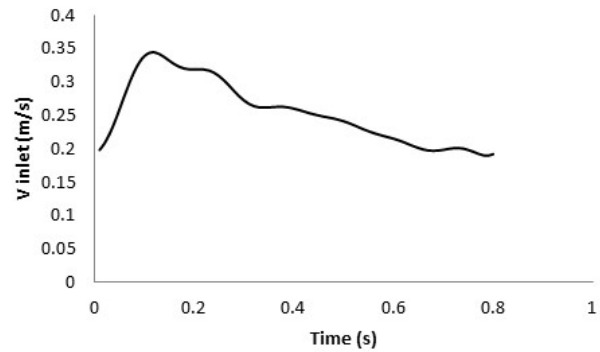


**Fig. 2.** Pulsatile velocity waveform used as velocity inlet

**Table 1.** Properties of vessel wall and blood

Vessel Wall	$\rho = 1060 \frac{kg}{m^3}$ , $\nu \approx 0.5$ , $E = 2.2$ Mpa, $t = 0.2$ mm
Blood	$\rho = 1050 \frac{kg}{m^3}$ , $\eta = 0.0035$ Pa s

time-step. To eliminate the initial effects of transient flow, computation is carried out for 3 periods, and at the third period the results were presented.

**Wall deformation**

In Fig. 3 total mesh displacement at the peak systole velocity for three different angles of 60°, 75° and 90° is presented. Flow is non-Newtonian in all three models. Since the vessel lies on the heart, it has fewer degrees of freedom along normal direction. Upper wall of the non-planar branch has more displacement to upward. Displacement of the non-planar branch due to its curvature is greater than its counterpart, the planar branch, which leads to reductions in wall shear stress in elastic model than rigid model. Displacement of divergence point in the model with bifurcation angle of 60° is greater than that in other models.

**Flow patterns**

Fig. 4 illustrates the streamlines at peak systole velocity ( $t = 0.13$ s). As shown in Fig. 4, irregularities in the streamlines at the beginning of branches are big.

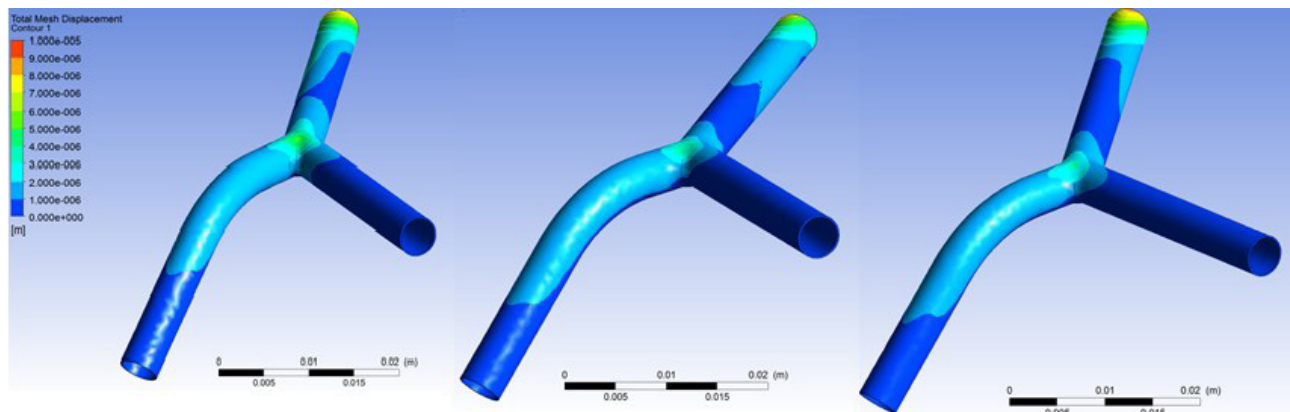


**Fig. 3.** Mesh displacement contour at peak of systole velocity

Fig. 5 demonstrates wall shear stress in 90° bifurcation with non-Newtonian fluid at three different times of heart beat. Fig. 4A, B and C are at the end of diastole, the peak of systole and the beginning of diastole, respectively. As shown in Fig. 5, wall shear stress at the outer walls of bifurcations is greatly reduced. Since the areas with low shear stresses are prone to stenosis, the outer walls of bifurcations in all models are potential areas for formation of atherosclerosis lesions.

Fig. 6 shows wall shear stresses along lines 1,2,3, and 4 in planar branch of 90° bifurcation angle at peak systole

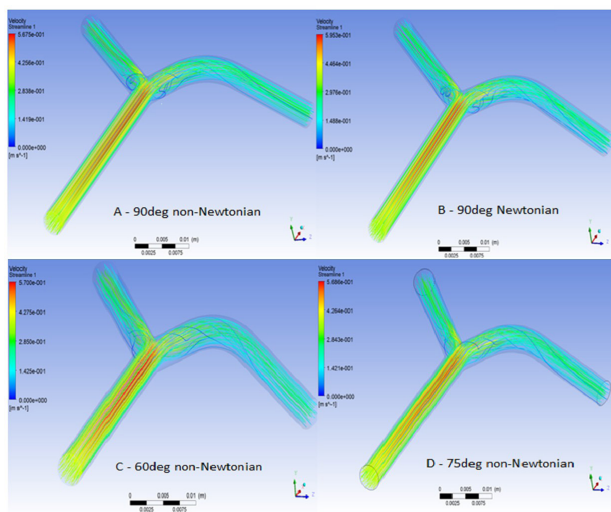


Fig. 4. Velocity streamlines at peak systole velocity

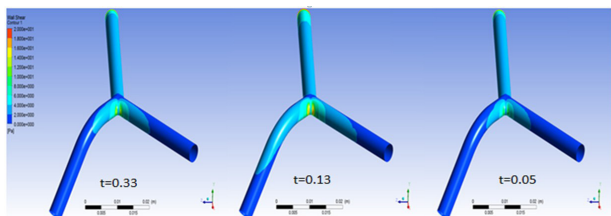


Fig. 5. Wall shear stress contours at 90° bifurcation angle, with non-Newtonian fluid

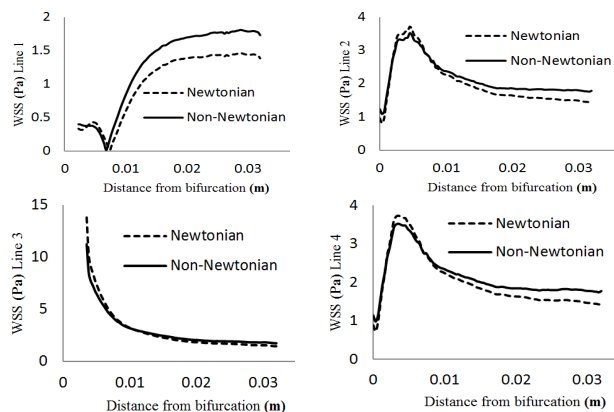


Fig. 6. WSS along lines 1, 2, 3 and 4 at 90° bifurcation angle at peak systole velocity

velocity (t=0.13). As shown in Fig. 6, wall shear stress in non-Newtonian fluid is greater than that in the Newtonian one. By going away from the onset of branches, shear stress along all four lines converge or diverge to a unique amount.

Fig. 7 gives the wall shear stress along line 7, on the outer wall of the non-planar branch at peak systole velocity (t=0.13). As it can be observed, wall shear stress in planar and non-planar branches almost have the same pattern. However, they differentiate in a way that in the curvature of non-planar branch a small reduction in wall shear stress is observed. This reduction amplifies the likelihood of atherosclerosis lesions in the curvature of non-planar branch.

**Bifurcation angle**

Bifurcation angle has a great impact on the velocity profile of branches. Fig. 8 depicts wall shear stresses along lines 1, 2, 3, and 4 in planar branch, at peak systole velocity. As it can be observed, shear stress at outer, lower, and upper walls of bifurcation rises with the increase of the bifurcation angle. But at the inner wall of bifurcation, wall shear stress falls down with the increase of bifurcation angle. Since stenosis mostly occurs at the outer walls of bifurcations, it can be concluded that the model with the bifurcation angle of 60° is more prone to stenosis than two other models. But the risk of atherosclerosis in inner walls of bifurcations is more than that in two other aforementioned models.

**Discussion**

Previously, we have performed numerical investigation of pulsatile blood flow in a bifurcation model with a non-planar branch,<sup>21</sup> the blood flow behavior in the circle of Willis,<sup>22</sup> blood flow coronary artery with consecutive stenosis and coronary-coronary bypass,<sup>23</sup> and also looked at the Possibility of atherosclerosis in an arterial bifurcation model.<sup>24</sup> In the current study, we investigated the blood flow in coronary artery bifurcation with a non-planar branch. The vessel wall was considered to be linear elastic, in which non-Newtonian and Newtonian flow cases were taken into consideration for modeling. We

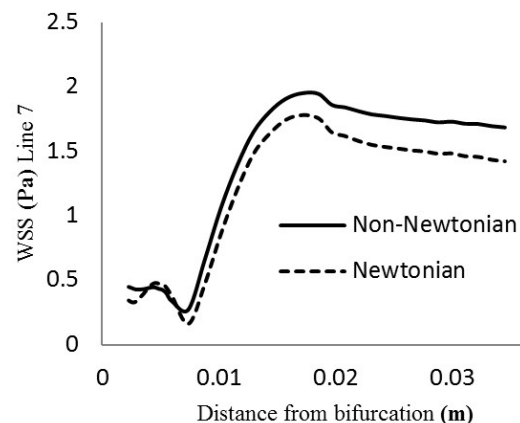
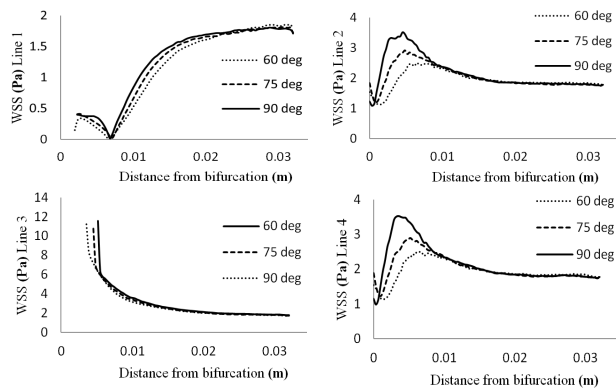


Fig. 7. WSS along line 7 in 90° bifurcation angle at peak systole velocity





**Fig. 8.** WSS along lines 1, 2, 3, and 4 at the peak systole velocity in models with bifurcation angles 60°, 75° and 90°

capitalized on the effects of wall compliance and non-Newtonian rheology of blood on characteristics of the flow while looking at the effect of bifurcation angle on flow behavior.

The results obtained from this research can help in the practical graft operation. It was found that the elasticity of vessel wall has a great impact on the hemodynamic characteristics of blood flow, especially in the non-planar branch. Due to the low displacement in planar branch, there are not any notable differences between the flow behavior in rigid and elastic walls. But in the non-planar branch, there are differences between the flow characteristics in elastic and rigid models. At the upper wall of the non-planar branch, wall shear stress was smaller than that in the rigid one. Lower wall shear stress was observed in the compliant wall than that in the rigid wall. The outer wall of bifurcation in all models had lower wall shear stress. In bifurcations with larger angles, wall shear stress was higher in outer walls, and lower in inner walls.

### Conclusions

Having compared the wall shear stress distribution for two Newtonian and non-Newtonian flows, significant differences were observed in both models. Velocity profiles in the Newtonian flow experiences a smaller gradient than its non-Newtonian counterpart. Higher wall shear stress distributions were observed in the non-Newtonian flow compared to the Newtonian flow. Outer walls of bifurcation in all models were identified as appropriate areas along with end of diastole as appropriate time for formation of plaques. Probability of stenosis in the non-planar bifurcation is higher than that in the planar branch due to the curvature of vessel. The compliant vessels are more prone to the stenosis than the rigid ones.

### Ethical issues

None to be declared.

### Competing interests

The authors declare no competing interests.

### References

1. Texon M. The hemodynamics concept of atherosclerosis. *Bulletin of the New York Academy of Medicine* **1960**;36:263-274.
2. Friedman MH, Barger CB, Deters OJ, Hutchins GM, Mark FF. Correlation between wall shear and intimal thickness at a coronary artery branch. *Atherosclerosis* **1987**;68:27-33.
3. Gibson CM, Diaz L, Kandarpa K. Relation of vessel wall shear stress to atherosclerotic progression in human coronary arteries. *ArteriosclerThromb* **1993**;13:310-5.
4. Nerem RM. Vascular fluid mechanics, the arterial wall and atherosclerosis. *Journal of Biomechanics* **1992**;114:274-82.
5. Nerem RM, Cornhill JF. The role of fluid mechanics in atherogenesis. *J Biomech* **1980**;102:181-9.
6. Ohja M, Ethier CR, Johnston KW, Cobbold RS. Steady and pulsatile flow fields in an end-to-side arterial anastomosis model. *J Vasc Surg* **1990**;12:747-53.
7. White SS, Zarins CK, Giddens DP, Bassiouny H, Loth F, Jones SA, et al. Hemodynamic patterns in two models of end-to-side vascular graft anastomoses: effects of pulsatility, flow division, Reynolds number, and hood length. *J Biomech Eng* **1993**;115:104-111.
8. Taylor CA, Hughes TJR, Zarins CK. Effect of exercise on hemodynamic conditions in the abdominal aorta. *J Vasc Surg* **1999**;29:1077-89.
9. Chen J, Lu XY. Numerical investigation of the non-Newtonian pulsatile blood flow in a bifurcation model with a non-planar branch. *J Biomech* **2006**;39:818-39.
10. Naruse T, Tanishita K. Large curvature effect on pulsatile entrance flow in a curved tube: model experiment simulating blood flow in an aortic arch. *J Biomech* **1996**;118:180-6.
11. Tanya S, Rokgers VG, Frazin LJ, Chandran KB. Numerical study on the secondary flow in the human aorta on local shear stresses in abdominal aortic branches. *J Biomech* **2000**;33:717-28.
12. Papaharilaoua Y, Poorly DJ, Sherwin SJ. The influence of out-of-plane geometry on pulsatile flow within a distal end-to-side anastomosis. *J Biomech* **2002**;35:1225-39.
13. Perktold K, Peter R. Numerical 3D-simulation of pulsatile wall shear stress in an arterial T-bifurcation model. *J Biomech* **1990**;12:1-12.
14. Prosi M, Perktold K, Ding Z, Friedman M H. Influence of curvature dynamics on pulsatile coronary artery flow in a realistic bifurcation model. *J Biomech* **2004**;37:1767-1775.
15. Sun Z, Chaichana T, Jewkes J. Computation of hemodynamics in the left coronary artery with variable angulations. *J Biomech* **2011**;44:1869-1878.
16. Leuprecht A, Perktold K, Prosi M, Berk T, Trubel W, Schima H. Numerical study of hemodynamics and wall mechanics in distal end-to-side anastomoses of bypass grafts. *J Biomech* **2002**;35:225-36.
17. Kabinejadianan F, Ghista DN. Compliant model of a coupled sequential coronary arterial bypass graft: Effects of vessel wall elasticity and non-Newtonian rheology on blood flow regime and hemodynamic parameters distribution. *Medical Engineering and Physics* **2012**;34:860-72.
18. Gradus-Pizlo I, Bigelow B, Mahomed Y, Sawada SG, Rieger K, Feigenbaum H. Left anterior descending coronary artery wall thickness measured by high frequency transthoracic and epicardial echocardiography includes adventitia. *J Cardiol* **2003**; 91:27-32.
19. Gijsen FJH, Van de Vosse FN, Janssen JD. The influence

- of the non-Newtonian properties of blood on the flow in large arteries: steady flow in a carotid bifurcation model. *J Biomech* **1999**;32:601-8.
20. Mulay AS, Computational modeling of cerebral aneurysm hemodynamics: effects of stenting. State University of Sunny Buffalo, **2002**.
  21. Arjmandi Tash O, Razavi SE. Numerical investigation of pulsatile blood flow in a bifurcation model with a non-planar branch: the effect of different bifurcation angles and non-planar branch. *Bioimpacts* **2012**; 2: 195-205. doi: 10.5681/bi.2012.023
  22. Razavi SE, Sahebjam R. Numerical Simulation of the blood flow behavior in the circle of Willis. *Bioimpacts* **2014**; 4: 89-94. doi: 10.5681/bi.2014.008
  23. Razavi SE, Zambouri R, Arjmandi-Tash O. Simulation of blood flow coronary artery with consecutive stenosis and coronary-coronary bypass. *Bioimpacts* **2011**; 1: 99-104. doi: 10.5681/bi.2011.013
  24. Arjmandi-Tash O, Razavi SE, Zambouri R. Possibility of atherosclerosis in an arterial bifurcation model. *Bioimpacts* **2011**; 1: 225-8. doi: 10.5681/bi.2011.032